V European Conference on Computational Fluid Dynamics
ECCOMAS CFD 2010
J. C. F. Pereira and A. Sequeira (Eds)
Lisbon, Portugal,14-17 June 2010

# RECENT DEVELOPMENTS ON HIGH-ORDER MULTIDIMENSIONAL UPWIND RESIDUAL DISTRIBUTION FOR EQUATIONS WITH VISCOUS TERMS

**Tiago Quintino*, Nadge Villedieu†, Herman Deconinck††**

von Karman Institute for Fluid Dynamics, Chaussee de Waterloo 72, 1640 Rhode-St-Genese,
e-mail: * quintino@vki.ac.be † villedie@vki.ac.be †† deconinck@vki.ac.be

**Key words:** CFD, high-order, residual distribution, viscous terms

**Abstract.** *We construct a $3^{rd}$ order multidimensional upwind residual distribution scheme for the system of Navier-Stokes equations. We divide $P^2$ finite elements into sub-elements, where we compute the quadratic residual in each sub-element and distribute it in a multi-dimensional upwind way to the downstream nodes. To discretise the viscous term, we look for a weight function that ensures equivalence between to a Petrov-Galerkin method for a scalar linear advection problem. The advective part of the conservation equation is discretised with a residual distribution scheme. The behavior of this high-order method is analysed on flows with high and low Reynolds number.*

## 1 Introduction

The goal of this work is to construct very high order ($3^{rd}$ order) Residual Distributive ($\mathcal{RD}$) schemes for systems of conservation laws ($\mathcal{CL}$) that include viscous terms. We focus on multidimensional upwind RD schemes for the solution of hyperbolic systems of equations. Their main advantages are:

- That $\mathcal{RD}$ schemes are designed for unstructured grids therefore handle well complex geometries.
- That these schemes are *multidimensional upwinding* ($\mathcal{MU}$), rendering the solution less dependent on the regularity and direction of the mesh. This marks a difference from many other methods like Finite Volume (FV) or Discontinuous Galerkin (DG) method, which are split by dimensions and are based on the solution of quasi 1D Riemann problems across element interfaces. $\mathcal{MU}$ reduces streamline cross diffusion yielding a higher resolution for similar number of degrees of freedom (DOFs).
- The schemes' multidimensional dissipation avoids any tuning of the artificial dissipation as in stabilised Finite Element method ($\mathcal{FE}$).

- The schemes' residual property provides a framework for high order schemes constructed on arbitrary unstructured meshes. It also features a compact stencil that makes code parallelization simpler.

Since viscosity is an isotropic phenomenon, upwinding is not the optimal way to discretise it and central schemes are usually used to discretize viscous terms. Traditionally in $\mathcal{RDS}$, the strategy is not much different. The common approach is to discretise the viscous part by a Galerkin method.

Unfortunately, when using quadratic elements, this discretization is not consistent and leads to a scheme that does not converge. For this reason, it is necessary to find a scheme that is consistent with the discretisation of the convective part and that is in agreement with the physical property of viscosity. A natural way to descretize the viscous term would be to include it in the residual and distribute together with the converctive part. Unfortunately this is not possible to compute because the residual involves second order derivatives of the unknowns, which for some shape functions are null.

One possible solution to this problem is described in [1] for the solution of the scalar advection-diffusion. There, the author uses the gradient of the solution as an unknown resulting in a first order system of equations which is solved by a residual distribution schemes. This methodology is also used by other methods such as DG [2] or spectral finite-volume method [3].

We present a different approach. We build a continuous weight function such that $\mathcal{RDS}$ and $\mathcal{PG}$ are equivalent on a linear advection problem. Then, the convective part is discretised by $\mathcal{RD}$ and the viscous part by $\mathcal{PG}$. In the first section, we describe the framework of residual distribution schemes for hyperbolic equations. Then, in the second section we link $\mathcal{RD}$ and $\mathcal{PG}$ methodologies by designing a weight function such that both formulations are equivalent. This weight function is used in the third section to extend $\mathcal{RD}$ to the discretisation of viscous terms. The last section is dedicated to the performance of these schemes. In particular, we show the improvements brought by the quadratic discretisation of the solution (compared to a linear discretisation).

## 2 High order RD schemes for hyperbolic conservation laws

We first present the design of high order upwind schemes for systems of hyperbolic conservation laws given by the form

$$\vec{\nabla} \cdot \mathcal{F}(\mathbf{U}) = 0 \quad \forall (x, y) \in \Omega \tag{1}$$

where $\mathbf{U}$ is the $m$-vector of the conserved quantities, and $\mathcal{F}$ is a $m \times 2$-tensor: $\mathcal{F} = (\mathbf{f^x}, \mathbf{f^y})$($\mathbf{f^x}$ and $\mathbf{f^y}$ being $m$-vectors).

### 2.1 Generalities and notations

For a given domain $\Omega$ we denote by $\tau_h$ a generic triangulation of $\Omega$ composed of a set of non-overlapping triangles $T \in \tau_h$. The elements of this triangulation are $P^k$ finite

elements. Each element is equipped with

$$M = \frac{(k+1)(k+2)}{2}$$

degrees of freedom as plotted on figure 1. These elements $T \in \tau_h$ form a continuous polynomial basis over the domain $\Omega$. Moreover, we sub-triangulate each triangle with a $P^1$ conformal triangulation. This means that $\forall\, k \geq 1$ on a given $T \in \tau_h$ we introduce $N = k^2$ sub-elements that we denote by $\{T_s\}_{s=1,N}$ sub-triangles in $T$.

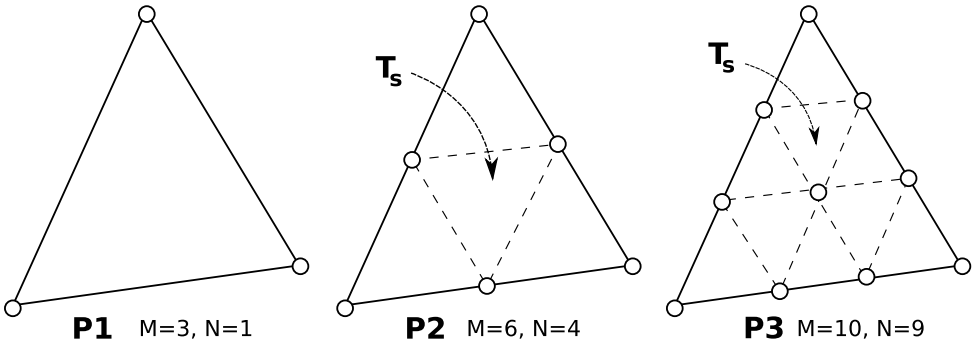


**Figure 1:** Sub-triangulations of Lagrangian elements

The solution is approximated by:

$$\mathbf{U}^h = \sum_{i \in \tau_h} \psi_i^{P^k}\, \mathbf{U}_i \;, \tag{2}$$

where $\psi_i^{P^k}$, the basis function of node $i$, is a continuous piecewise polynomial of order $k$ and $\mathbf{U}_i$ is defined by $\mathbf{U}_i = \mathbf{U}^h(x_i, y_i)$.

On each $T \in \tau_h$ we also consider the set of vectors $\{\vec{n}_j\}_{j \in T}$, defined by the inward normals to the edges of $T$ facing each node $j \in T$. In the general $P^k$ case, with $k > 1$, we will assume that the $\vec{n}_j$'s are defined on a local sub-element $T_s \in T$, as shown on figure 2 for the case $k = 2$. Finally, on each sub-element we define the following upwind parameters:

$$K_j = \frac{1}{2} \frac{\partial \mathcal{F}(\mathbf{U}^*)}{\partial \mathbf{U}} \cdot \vec{n}_i \tag{3}$$

where $\mathbf{U}^*$ is a suitable arbitrary average of $\mathbf{U}$.

The residual distribution scheme consists of three steps:

1. Computation of the residual on each sub-element:

$$\mathbf{\Phi}^{T_s} = \int_{T_s} \nabla \cdot \mathcal{F}\, d\Omega = \oint_{\partial T_s} \mathcal{F}\, d\vec{l} \tag{4}$$

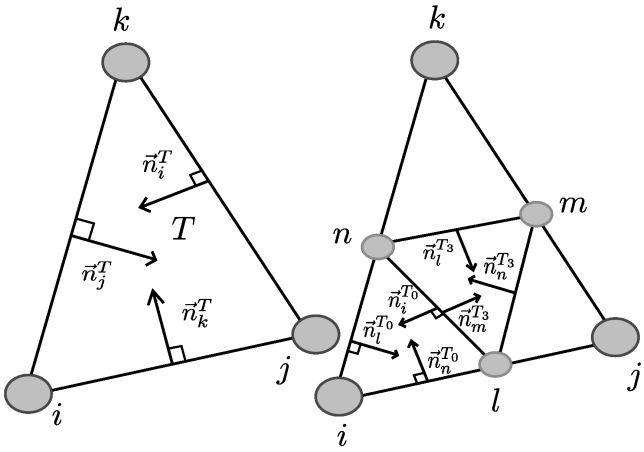


**Figure 2:** Definition on the inward normals $\vec{n}_i$

2. Distribution of the residual to each node of the sub-element:

$$\mathbf{\Phi}_i^{T_s} = B_i^{T_s} \mathbf{\Phi}^{T_s} \tag{5}$$

3. Resolution of a system of nodal equations:

$$\sum_{i,\in T_s} \mathbf{\Phi}_i^{T_s} = 0 \tag{6}$$

This system can be solved by pseudo-time ($\tau$) iterations:

$$\frac{\partial \mathbf{U}}{\partial \tau} - \sum_{i \in T_s} \mathbf{\Phi}_i^{T_s} = 0 \tag{7}$$

For example, we can solve (7) by an explicit forward-Euler method:

$$\mathbf{U}_i^{\kappa+1} = \mathbf{U}_i^{\kappa} + \frac{\Delta\tau}{C_i} \left( \sum_{i \in T_s} \mathbf{\Phi}_i^{T_s} \right)^{\kappa} \tag{8}$$

where $C_i$ represents a scaling of the pseudo-time, such that a CFL-type condition is verified. It is also possible to solve (7) using an implicit solver:

$$\frac{\mathbf{U}_i^{\kappa+1} - \mathbf{U}_i^{\kappa}}{\Delta\tau} = \left( \sum_{i \in T_s} \mathbf{\Phi}_i^{T_s} \right)^{\kappa+1} \tag{9}$$

In the hyperbolic case, the schemes we consider are a particular case of the $\mathcal{RD}$ schemes introduced by Abgrall [4].

### 2.2 Properties of the schemes

We are interested in schemes with the following properties.

#### 2.2.1 Multidimensional Upwind ($\mathcal{MU}$)

We can use the sign of the eigenvalues of $K_i$ to send a smaller or bigger part of the residual to each nodes of the sub-element to build a multidimensional upwind scheme. A matrix scheme is $\mathcal{MU}$ if

$$K_i^+ = 0 \Rightarrow \mathbf{\Phi}_i^{T_s} = 0 \text{ with } K_i^+ = R_i \Lambda_i^+ R_i^{-1} \tag{10}$$

where $R_i$ and $\Lambda_i$ are respectively the matrices of the right eigenvectors and eigenvalues of $K_i$. This property is very usefull for problems involving advective phenomenona because the distribution of the residual follows the physical flow which reduces cross-diffusion and improves global accuracy.

But, when an isotropic phenomenon such as viscosity is involved the construction of such scheme becomes more difficult. The goal of this work is to present the way to handle this within the $\mathcal{RD}$ framework.

#### 2.2.2 Linearity Preservation ($\mathcal{LP}$) and accuracy

The non-linearity of $\mathcal{F}$ may introduce some solution discontinuities and some physical instabilities that make the problem harder to solve. It is also necessary to have a stable scheme that is also accurate enough. A scheme is of $r$-th order accurate if

$$\mathbf{\Phi}_i^{T_s} = \mathcal{O}(h^{r+1})$$

in particular, if the solution is discretised by a $k$-th order approximation ($P^k$ elements), since

$$\mathbf{\Phi}^{T_s} = \mathcal{O}(h^{k+2})$$

and $\mathbf{\Phi}_i^{T_s} = B_i \mathbf{\Phi}^{T_s}$, it is necessary that $B_i$ is uniformly bounded to get a scheme of order $k+1$. In this article, we will use the upwinding scheme called LDA.

### 2.3 LDA scheme

LDA is a low diffusion scheme that has the property that on a scalar advection flow aligned with the mesh the inlet state is exactly perserved. The distribution matrix of LDA is defined by:

$$B_i^{LDA} = K_i^+ \left( \sum_{j \in T_s} K_j^+ \right)^{-1} \tag{11}$$

This scheme is upwind with $(k+1) - th$ order accuracy.

### 2.4 Equivalence with Petrov-Galerkin method ($\mathcal{PG}$)

Having described the design of high order $\mathcal{RD}$ schemes, we will link the $\mathcal{RD}$ formulation with the $\mathcal{PG}$ schemes. In both methods the solution is discretised by combination of the continuous Lagrangian basis functions. However, upwind $\mathcal{RD}$ schemes such as LDA were developed for hyperbolic conservation laws whereas $\mathcal{PG}$ can be used for more general conservation laws. Therefore, one idea to extend upwind $\mathcal{RD}$ to viscous terms is to use a Petrov-Galerkin approach. To do so, we need to find a weight function such that $\mathcal{RD}$ and $\mathcal{PG}$ schemes are equivalent for hyperbolic conservation laws. Without loss of generality we consider the linear scalar advection equation:

$$\vec{a} \cdot \nabla u = 0 \tag{12}$$

Lets look for the weight function $\omega_i^{P^k}$ such that if $u$ is linear on each sub-element $\mathcal{PG}$ and $\mathcal{RD}$ method would be equivalent. Then, we have:

$$\begin{cases} B_i^{T_s} \displaystyle\int_{T_s} \vec{a} \cdot \nabla u \, d\Omega &= \displaystyle\int_{T_s} \omega_i^{P_k} \vec{a} \cdot \nabla u \, d\Omega \quad \text{if } i \in T_s \\ 0 &= \displaystyle\int_{T_s} \omega_i^{P_k} \vec{a} \cdot \nabla u \, d\Omega \quad \text{if } i \notin T_s \end{cases} \tag{13}$$

This yields the following conditions:

$$\begin{cases} \displaystyle\int_{T_s} \omega_i^{P_k} \, d\Omega &= B_i^{T_s} |T_s| \quad \text{if } i \in T_s \\ \displaystyle\int_{T_s} \omega_i^{P_k} \, d\Omega &= 0 \qquad\quad \text{if } i \notin T_s \end{cases} \tag{14}$$

A weight function that verifies these conditions is:

$$\omega_i^{P_k}{}_{|_{T_s}} = \psi_i^{P_k} + \alpha_i^{T_s} S^{T_s} \tag{15}$$

where $S^{T_s}$ is the bubble function (figure 3) of the sub-element $T_s$:

$$S^{T_s}(x,y) = \begin{cases} 0 \text{ if } (x,y) \in \partial(T_s) \\ 1 \text{ if } (x,y) = (x_g, y_g) \end{cases} \tag{16}$$

$(x_g, y_g)$ being the gravity centre of the sub-element $T_s$.
Finally, $\alpha_i^{T_s}$ is defined by:

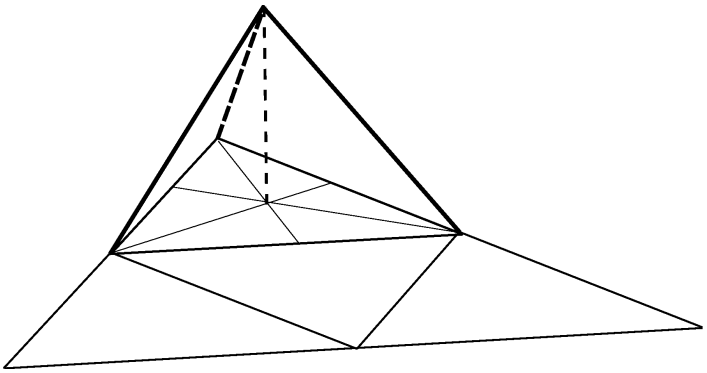

**Figure 3:** Bubble function

$$\alpha_i^{T_s} = \begin{cases} \dfrac{B_i^{T_s}|T_s| - \displaystyle\int_{T_s} \psi_i^{P_k}\, d\Omega}{\displaystyle\int_{T_s} S^{T_s}\, d\Omega} & \text{if } i \in T_s \\ \dfrac{-\displaystyle\int_{T_s} \psi_i^{P_k}\, d\Omega}{\displaystyle\int_{T_s} S^{T_s}\, d\Omega} & \text{if } i \notin T_s \end{cases} \tag{17}$$

Compared to the shape functions $\psi_i^{P_k}$, the local regularity (within $T$) of the bubble function $S^{T_s}$ is quite low. However, ultimately both shape and bubble functions are in the same functional space $H_0^1(\Omega)$ and share simple $C^0$ continuity. In the next section, we use this weight function to construct a consistent scheme to solve systems of conservation laws with viscous terms.

## 3 Extension to viscous terms

We consider the solution of a system of conservation laws with viscous terms:

$$\vec{\nabla} \cdot \mathcal{F}(\mathbf{U}) = \nabla \cdot (\nabla \mathcal{G}(\mathbf{U})) \quad \forall (\mathbf{x}, \mathbf{y}) \in \mathbf{\Omega} \tag{18}$$

To construct a consistent $\mathcal{RD}$ scheme to solve equation (18), we use the $\mathcal{PG}$ formulation of the last section:

$$\mathbf{\Phi}_i^{PG,T} = \sum_{T_s \in T} \underbrace{\int_{T_s} \omega_i^{PG} \vec{\nabla} \cdot \mathcal{F}(\mathbf{U}) d\Omega}_{I} + \underbrace{\int_{T_s} \nabla \omega_i^{PG} \nabla \mathcal{G}(\mathbf{U}) d\Omega}_{II} \tag{19}$$

We previously saw that integral $I$ is equivalent to $\mathcal{RD}$ so we will replace it by the nodal residual of $\mathcal{RD}$ method. Finally, the nodal residual of the $\mathcal{RD}$ is:

$$\begin{cases} \mathbf{\Phi}_i^{T_s} = & B_i \oint_{\partial T_s} \mathcal{F}(\mathbf{U}) d\Omega & + \int_{T_s} \nabla \omega_i^{PG} \nabla \mathcal{G}(\mathbf{U}) d\Omega & i \in T_s \\ \mathbf{\Phi}_i^{T_s} = & 0 & + \int_{T_s} \nabla \omega_i^{PG} \nabla \mathcal{G}(\mathbf{U}) d\Omega & i \notin T_s \end{cases} \tag{20}$$

After assembling all the contributions, we get the following system to solve:

$$\sum_{T, i \in T} \sum_{T_s, T_s \in T} \mathbf{\Phi}_i^{T_s} = 0 \tag{21}$$

With this method we achieve $(k+1)$ order scheme on $P^k$ elements. We denote by LDA($P^k$), the schemes when using a such $P^k$ discretisation.

**Remark:** In [6], the authors explained that in the case of scalar advection-diffusion, to keep an uniform order of accuracy, it is necessary to add a finite element stabilisation. However, in this work we do not use it because in [7] it is shown that in the case of Navier-Stokes equations, for Reynolds number above 100, the stabilisation is not necessary.

## 4 Results

### 4.1 Navier-Stokes system of equations

We will test the performance of our method by discretising the Navier-Stokes equations and analysing the its solution of a series of testcases:

$$\frac{\partial \mathbf{U}}{\partial t} + \vec{\nabla} \cdot \mathcal{F}(\mathbf{U}) = \vec{\nabla} \cdot \mathcal{G} \text{ on } \Omega \tag{22}$$

where $\mathbf{U}$ is the vector of conservative variables and $\mathcal{F} = (\mathbf{f}^x, \mathbf{f}^y)$ the convective flux. Their definitions are:

$$\mathbf{U} = \begin{pmatrix} \rho \\ \rho u \\ \rho v \\ \rho E \end{pmatrix}, \mathbf{f}^x(\mathbf{U}) = \begin{pmatrix} \rho u \\ \rho u^2 + p \\ \rho uv \\ \rho H u \end{pmatrix}, \mathbf{f}^y(\mathbf{U}) = \begin{pmatrix} \rho v \\ \rho uv \\ \rho v^2 + p \\ \rho H v \end{pmatrix},$$

where $\rho$ is the density, $(u, v)$ the velocity and $p$ the pressure. $E$ and $H$ are the total energy per unit of mass and the enthalpy. They are related to the other variables by equation (23):

$$H = E + \frac{p}{\rho} \quad , \quad E = \frac{p}{(\gamma - 1)\rho} + \frac{1}{2}(u^2 + v^2) \tag{23}$$

where $\gamma$ is the adiabatic exponent, equal to $\frac{7}{5}$ for air. With $\tau$ being a linear function of the velocity gradient and $\mu$ is the molecular viscosity coefficient, the definition of the viscous flux is given by equations (24) and (25):

$$\mathcal{G}^x = \begin{pmatrix} 0 \\ \tau_{xx} \\ \tau_{xy} \\ u\tau_{xx} + v\tau_{xy} - \frac{\partial q}{\partial x} \end{pmatrix}, \mathcal{G}^y = \begin{pmatrix} 0 \\ \tau_{xy} \\ \tau_{yy} \\ u\tau_{xy} + v\tau_{yy} - \frac{\partial q}{\partial y} \end{pmatrix} \tag{24}$$

$$\tau_{xx} = \mu\left(\frac{4}{3}\frac{\partial u}{\partial x} - \frac{2}{3}\frac{\partial v}{\partial y}\right), \tau_{yy} = \mu\left(\frac{4}{3}\frac{\partial v}{\partial y} - \frac{2}{3}\frac{\partial u}{\partial x}\right), \tau_{xy} = \mu\left(\frac{\partial u}{\partial y} + \frac{\partial v}{\partial x}\right) \tag{25}$$

The heat flux is modeled according to Fourier's law, equation (26), where $\kappa$ is the thermal conductivity coefficient.

$$q_{x_j} = -\kappa\frac{\partial T}{\partial x_j} \tag{26}$$

### 4.2 Flow over a cylinder: $Re = 40, M = 0.2, \alpha = 0$

We consider a test case with a low Reynolds number flow. This test case was performed on two meshes, the finest one composed of 44312 degrees of freedom and the coarsest composed of 4080. The solution on the finest mesh with LDA($P^1$) will be used as a reference solution. On figures 4 and 5 we plot the Mach number iso-lines and the streamlines. These plots show little difference between LDA($P^1$) and LDA($P^2$).

The advantage of the LDA($P^2$) quadratic discretisation is more obvious on the plot of the skin friction on figure 6. There, we plot the skin friction on the cylinder in function of the angle measuring the position of a point on the cylinder: 0° represents the leading edge and 180° the trailing edge. The maximum of $C_f$ is closer to the reference one, when using quadratic discretisation. Finally, we can see on figure 7 that both schemes converge well to machine accuracy.

### 4.3 Flow over a NACA-0012: $Re = 5000, M = 0.5, \alpha = 0$

We consider the flow over a NACA-0012 at Mach 0.5 and Reynolds 5000 without angle of incidence. For this test case the Reynolds number is close to the limit of steady laminar flow. The solution has a characteristic separation of the flow near the trailing edge. This forms two symmetrical recirculation bubbles in the near-wake region of the airfoil. The Mach number iso-lines computed using the quadratic discretisation are plotted in figure 9. This solution was obtained on a non-symetrical mesh plotted (see figure 8) which has 8564 DOFs (nodes on the mesh), from which 200 are on the airfoil. We also plot the distribution of pressure coefficient $C_p$ (figure 11) and of the friction coefficient $C_f$ (figure 10) around the arifoil. These plots show that we obtain a symetrical result.

On figure 12, we compare the results obtained by LDA($P^1$) and LDA($P2$) on meshes having the same number of degrees of freedom. The recirculation bubbles are resolved by the two schemes. We can see that the recirculation is not symmetrical when using a linear LDA($P^1$) discretisation of the solution, because the scheme is sensitive to the asymmetry

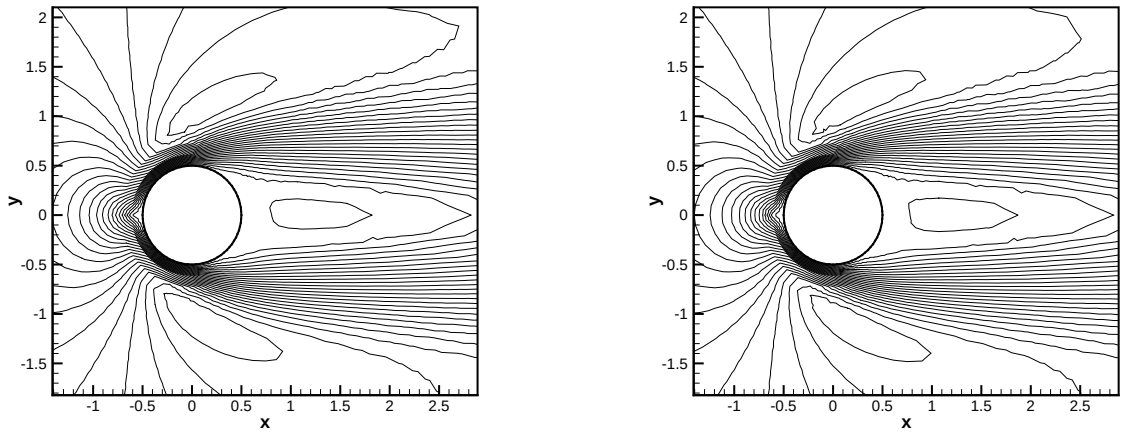


**Figure 4:** Viscous cylinder: Mach number iso-lines ($\Delta M = 0.02$) on the coarse mesh using LDA($P^1$) (left) and LDA($P^2$) (right)

of the mesh. In the case of a quadratic LDA($P2$) discretisation the recirculations are perfectly symmetrical. On figure 13, we see that both schemes converge well to machine accuracy and with almost the same number of iterations.

On table 1, we compare the drag coefficient and the separation points of literature to the ones obtained with LDA. It is difficult to drive any conclusion from the pressure drag $C_{d,p}$ because the values obtained with LDA($P^1$) and LDA($P^2$) are very similar. Concerning the viscous component, already with the second mesh we obtain with LDA($P^2$) a value very close to the literature, whereas with LDA($P^1$) even for the finest mesh the values are far from the references. Similarly, on the coarsest meshes, we obtain a good computation of the separation point when using LDA($P^2$), whereas with the LDA($P^1$) even for the finest mesh the result is far from the expected result.

Finally, some comments on efficiency: to run the LDA($P^2$) $3^{rd}$ order scheme on a coarse mesh, 682s time were necessary. To obtain a similar result with the LDA($P^1$) $2^{nd}$ order scheme it is necessary to use a finer mesh which it takes 2272s. Although this is not a rigorous comparison, it appears to support the assumption that it is faster, for the same accuracy threshold, to obtain a result with the high order $P^2$ scheme than with the $P^1$ low order scheme.

## 5 Conclusion

We have presented the extension of high order upwind Residual Distribution schemes to the Navier-Stokes system of equations. We have shown the capability of LDA($P^2$) for these flows, and in particular, we have shown the advantage of the LDA($P^2$) discretization over the LDA($P^1$), both in terms of accuracy and performance.

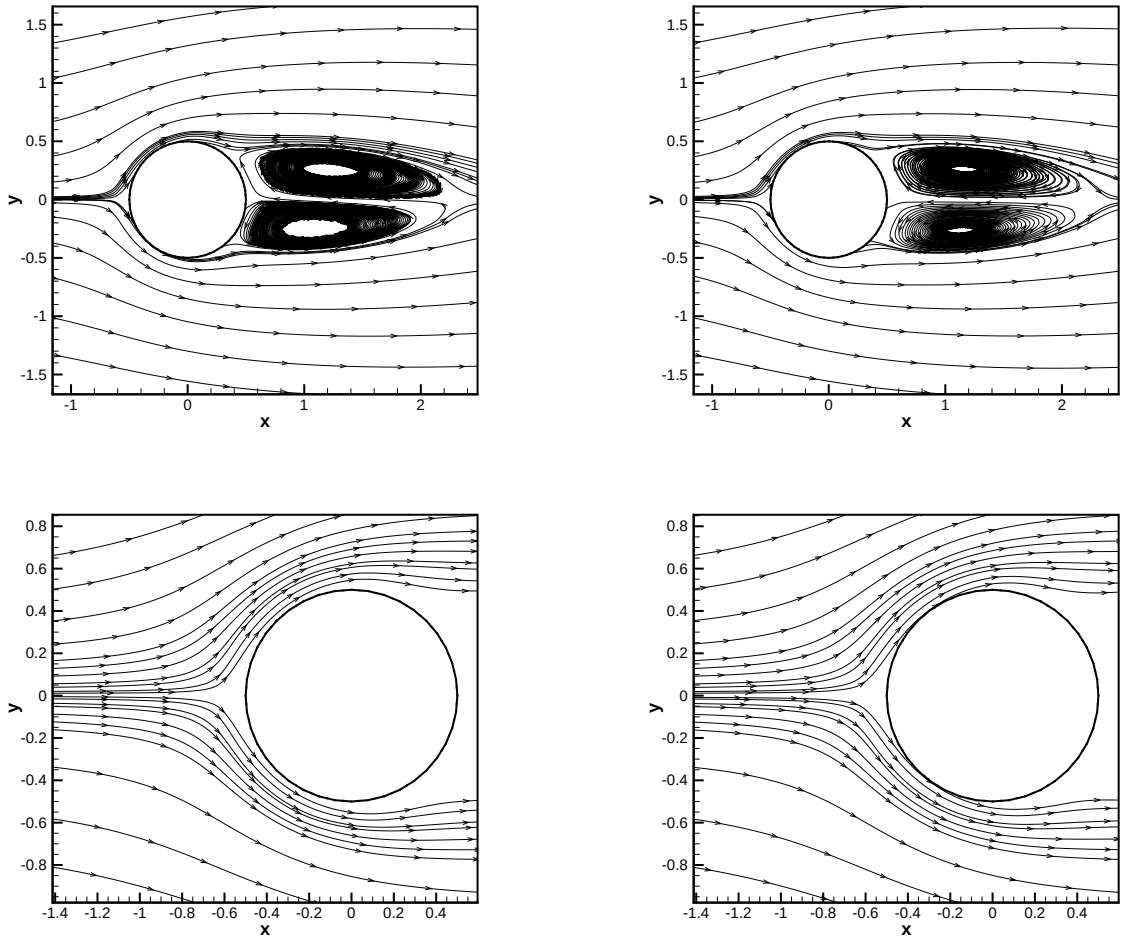


**Figure 5:** Viscous cylinder: Streamlines on the coarse mesh using LDA($P^1$) (left) and LDA($P^2$) (right)

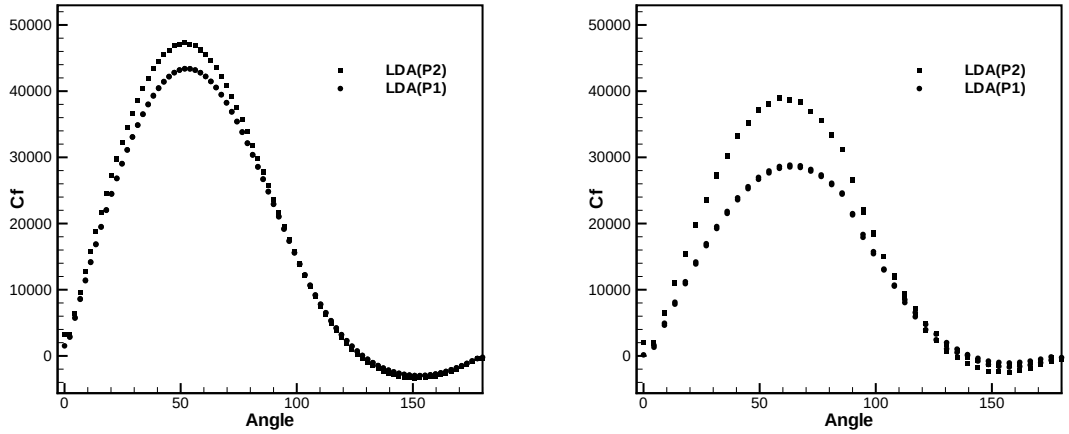


**Figure 6:** Viscous cylinder: Skin friction of LDA($P^1$) and LDA($P^2$) for the fine mesh (left) and the coarse one (right)

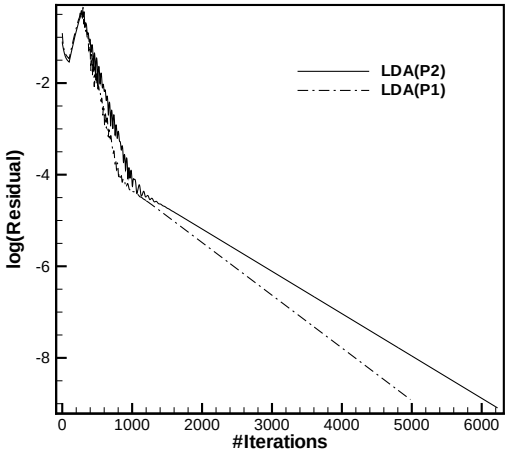


**Figure 7:** Viscous cylinder: Convergence history of implicit newton iterator for LDA($P^1$) and LDA($P^2$)

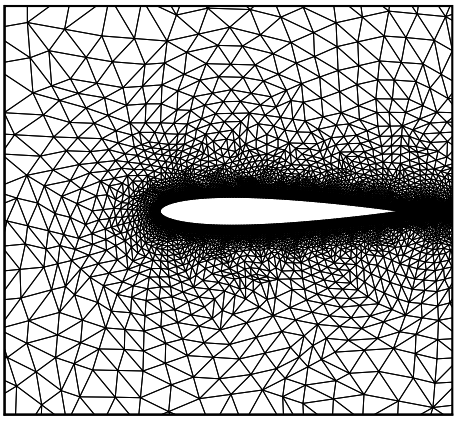

**Figure 8:** Viscous flow over a NACA-0012: Type of mesh used

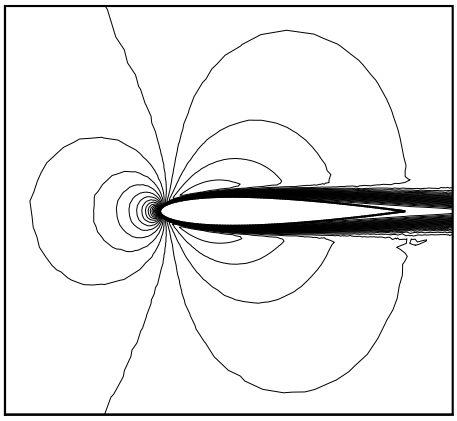

**Figure 9:** Viscous flow over a NACA-0012: Mach number iso-lines ($\Delta M = 0.02$)

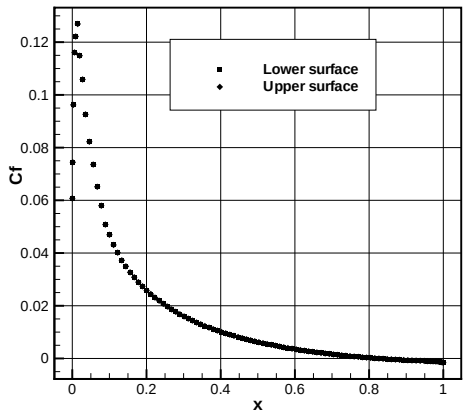


**Figure 10:** Skin friction coefficient

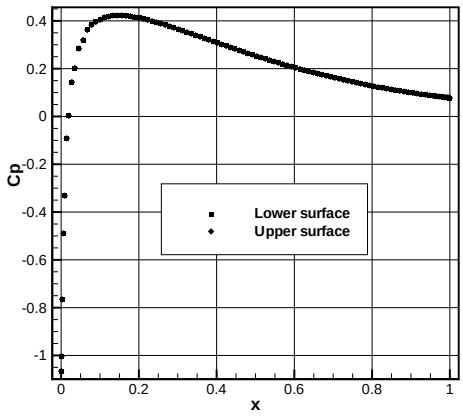


**Figure 11:** Pressure coefficient

## REFERENCES

[1] Nishikawa, H.: A first order system approach for diffusion equation. I:Second-order residual distribution schemes. *J. of comp. phys.*, **227**, 315–352 (2007).

[2] Bassi F., Rebay S. :A high-order accurate discontinuous finite element method for the numerical solution of the compressible Navier-Stokes equations *Journal of computational physics*, **131**, 267-279 (1997)

[3] Sun, Y., Wang, Z.J., Liu, Y. : Spectral (finite) volume method for conservation laws on unstructured grids VI: Extension to viscous flow *Journal of computational physics*,

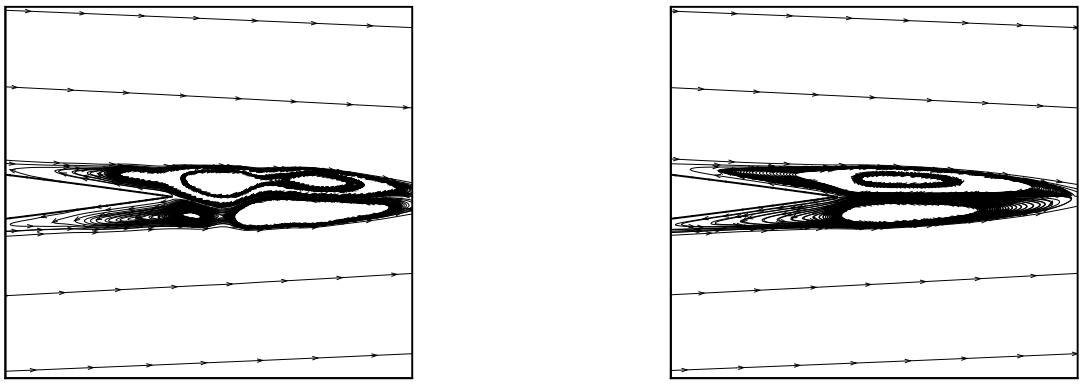

**Figure 12:** Viscous flow over a NACA-0012: streamlines, zoom in on the re-circulations using LDA($P^1$) (left) and LDA($P^2$) (right)

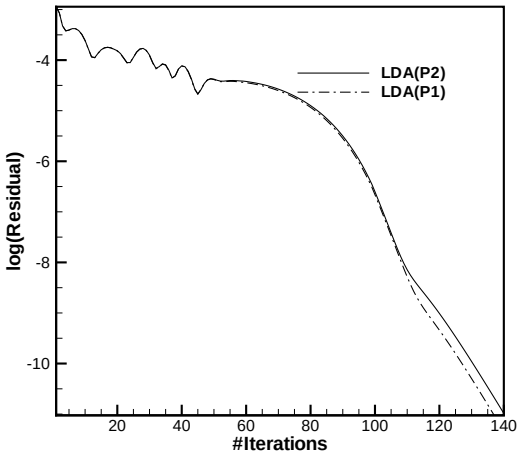


**Figure 13:** Viscous flow over a NACA-0012: Convergence history of implicit newton iterator for LDA($P^1$) and LDA($P^2$)

**215**, 41–58 (2006)

[4] Abgrall, R., Roe, P.L.: High order fluctuation schemes on triangular meshes. J. Sci. Comput., **19(3)**, 3–36 (2003)

[5] van der Weide E. *Compressible Flow Simulation on Unstructured Grids using Multi-*

| Mesh | Cdp | Cdv | Separation point |
|---|---|---|---|
| 4630 DOF (148 on wall) $P^1$ | 0.02239 | 0.03132 | 94.5 |
| 4630 DOF (148 on wall) $P^2$ | 0.02238 | 0.03414 | 82.5 |
| 8564 DOF (200 on wall) $P^1$ | 0.02296 | 0.03130 | 87 |
| 8564 DOF (200 on wall) $P^2$ | 0.02234 | 0.03294 | 82.3 |
| 17146 DOF (300 on wall) $P^1$ | 0.02284 | 0.03181 | 82.9 |
| 17146 DOF (300 on wall) $P^2$ | 0.02239 | 0.03274 | 82.1 |
| Reference [8] 16384 | 0.0219 | 0.0337 | 81.9 |
| Reference [9] 65536 | 0.0227 | 0.0327 | 81.4 |
| Reference [2] 1024 (cubic elements) | 0.02208 | 0.03303 | |

**Table 1:** Comparison of Drag coefficients and separation point with literature

*dimensional Upwind Schemes*, Techische Universiteit Delft, 1998

[6] Ricchiuto, M., Villedieu, N., Abgrall, R. and Deconinck, H.: On uniformly high order accurate residual distribution schemes for advection-diffusion. *J. Computational and Applied Mathematics*, **215**, 547–556 (June 2007)

[7] Ricchiuto, M., Dobes, J., Villedieu, N. and Abgrall, R.: On uniformly high-order accurate residual distribution schemes for advection-diffusion, *Journal of Computational and Applied Mathematics*, **215(2)**, 547–556, (2006)

[8] Martinelli L., *Calculations of Viscous Flows with a Multigrid Method*, Ph.D. thesis, Dept. of Mechanical and Aerospace Engineering, Princeton University, 1987.

[9] Radespiel R. and Swanson R.C., "An Investigation of Cell Centered and Cell Vertex Multigrid schemes for the Navier-Stokes Equations" AIAA Paper No. 89-0453, 1989 (unpublished)